Basal Autophagy is altered in Lagotto Romagnolo Dogs with an ATG4D mutation

Syrjä, Pernilla; Anwar, Tahira; Pääkkönen, Tarja; Kyöstilä, Kaisa; Hultin Jäderlund, Karin ...

2017-11
SAGE Publications Ltd
http://hdl.handle.net/10138/297783
Syrjä, P, Anwar, T, Pääkkönen, T, Kyöstilä, K, Hultin Jäderlund, K, Cozzi, F, Rohdin, C, Hahn, K, Wohlsein, P, Baumgärtner, W, Henke, D, Oevermann, A, Sukura, A, Leeb, T, Lohi, H & Eskelinen, E-L 2017, 'Basal Autophagy is altered in Lagotto Romagnolo Dogs with an ATG4D mutation', Veterinary Pathology, vol. 54, no. 6, pp. 953-963. https://doi.org/10.1177/0300985817712793

Veterinary Pathology
2017, Vol. 54(6) 953-963

DOI: 10.1177/0300985817712793
journals.sagepub.com/home/vet

Basal Autophagy Is Altered in Lagotto Romagnolo Dogs with an *ATG4D* Mutation

Pernilla Syrjä[1], Tahira Anwar[2], Tarja Jokinen[3], Kaisa Kyöstilä[1,4,5], Karin Hultin Jäderlund[6], Francesca Cozzi[7], Cecilia Rohdin[8,9], Kerstin Hahn[10], Peter Wohlsein[10], Wolfgang Baumgärtner[10], Diana Henke[11], Anna Oevermann[11], Antti Sukura[1], Tosso Leeb[12], Hannes Lohi[1,4,5], and Eeva-Liisa Eskelinen[2]

Abstract

A missense variant in the autophagy-related *ATG4D*-gene has been associated with a progressive degenerative neurological disease in Lagotto Romagnolo (LR) dogs. In addition to neural lesions, affected dogs show an extraneural histopathological phenotype characterized by severe cytoplasmic vacuolization, a finding not previously linked with disturbed autophagy in animals. Here we aimed at testing the hypothesis that autophagy is altered in the affected dogs, at reporting the histopathology of extraneural tissues and at excluding lysosomal storage diseases. Basal and starvation-induced autophagy were monitored by Western blotting and immunofluorescence of microtubule associated protein 1A/B light chain3 (LC3) in fibroblasts from 2 affected dogs. The extraneural findings of 9 euthanized LRs and skin biopsies from 4 living affected LRs were examined by light microscopy, electron microscopy, and immunohistochemistry (IHC), using antibodies against autophagosomal membranes (LC3), autophagic cargo (p62), and lysosomal membranes (LAMP2). Biochemical screening of urine and fibroblasts of 2 affected dogs was performed. Under basal conditions, the affected fibroblasts contained significantly more LC3-II and LC3-positive vesicles than did the controls. Morphologically, several cells, including serous secretory epithelium, endothelial cells, pericytes, plasma cells, and macrophages, contained cytoplasmic vacuoles with an ultrastructure resembling enlarged amphisomes, endosomes, or multivesicular bodies. IHC showed strong membranous LAMP2 positivity only in sweat glands. The results show that basal but not induced autophagy is altered in affected fibroblasts. The ultrastructure of affected cells is compatible with altered autophagic and endo-lysosomal vesicular traffic. The findings in this spontaneous disease provide insight into possible tissue-specific roles of basal autophagy.

Keywords

basal autophagy, Western blot, immunofluorescence, electron microscopy, cytoplasmic vacuolization, pathology, *ATG4D*, dog

[1]Department of Veterinary Biosciences, Faculty of Veterinary Medicine, University of Helsinki, Helsinki, Finland
[2]Department of Biosciences, Faculty of Biological and Environmental Science, University of Helsinki, Helsinki, Finland
[3]Department of Equine and Small Animal Medicine, Faculty of Veterinary Medicine, University of Helsinki, Helsinki, Finland
[4]Department of Molecular Genetics, Folkhälsan Institute of Genetics, University of Helsinki, Helsinki, Finland
[5]Research Programs Unit, Molecular Neurology, University of Helsinki, Helsinki, Finland
[6]Department of Companion Animal Clinical Sciences, Norwegian University of Life Sciences, Oslo, Norway
[7]Clinica Neurologica Veterinaria, Milan, Italy
[8]Department of Clinical Sciences, Swedish University of Agricultural Science, Uppsala, Sweden
[9]Anicura, Albano Small Animal Hospital, Danderyd, Sweden
[10]Department of Pathology, University of Veterinary Medicine Hannover, Hannover, Germany
[11]Division of Neurological Sciences, Vetsuisse Faculty, University of Bern, Bern, Switzerland
[12]Institute of Genetics, Vetsuisse Faculty, University of Bern, Bern, Switzerland

Supplementary material for this article is available online.

Corresponding Author:
Pernilla Elisabet Sofia Syrjä, Department of Veterinary Biosciences, Faculty of Veterinary Medicine, University of Helsinki, Agnes Sjobergsgatan 2 PO Box 66 HELSINKI, FI 00014 Finland.
Email: pernilla.syrja@helsinki.fi

Autophagy is a cellular process responsible for lysosomal degradation of damaged or unnecessary organelles and aggregated long-lived proteins. It is active at low levels under basal conditions and can be upregulated during stressful situations, such as starvation.[23,24,26] Autophagy takes care of organelle turnover under basal conditions, provides nutrients for the cell under stress, and protects cells from damage caused by aggregate-prone proteins.[23,24] Alterations in degradative autophagic flow have been linked with disease processes, among them neurodegeneration.[13,17,22] Moreover, several cell- and tissue-specific functions of the autophagic pathway have been revealed. These include involvement in unconventional secretion of von Willebrand factor by endothelial cells,[32] release of specific cytokines from inflammatory cells,[6] and disposal of unspecific content through exocytosis of autophagic vacuoles,[30] which indicates that the autophagic membranes and machinery are not only active in degradative tasks. Basal and stress-induced autophagy may be differently regulated. It was recently shown that induced autophagy can function normally in cells deficient in basal autophagy[26,34] and that the substrates for basal autophagy differ from those of starvation-induced autophagy.[35]

When endogenous cytoplasmic material is degraded through macroautophagy (hereafter called autophagy), the cargo is first sequestered into a double membrane–bound cytoplasmic vacuole, the autophagosome, which then delivers the cytoplasmic cargo to lysosomes for degradation. The degradation occurs in a transient single membrane–bound organelle, the autolysosome, which develops through fusion of autophagosomes and lysosomes in a multistep maturation process. Alternatively, cytosolic protein can be directly engulfed by lysosomes in microautophagy[20] or transported into the lysosomal lumen through the lysosomal membranes in chaperone-mediated autophagy.[23]

The autophagic system acts in cross-talk with the endo-lysosomal degradation pathway of extracellular material.[7,19,26] During internalization of extracellular molecules, cells target the endocytic vesicle to the early endosome. From here, the content is alternatively delivered back to the plasma membrane in recycling endosomes or packed within the membrane-bound multivesicular body (MVB) that has 2 alternative destinations: It can deliver its cargo to the lysosome for degradation or the plasma membrane for exocytosis.[7,19] Membranous fusion and fission events occur within and between the endo-lysosomal and the autophagic pathways.[9,19] Autophagosomes can fuse with late endosomal vesicles or MVBs to form amphisomes: single membrane–bound vesicles that possess both autophagic and endo-lysosomal membrane markers and contain endogenous as well as exogenous material.[9] Finally, autophagosomes or amphisomes fuse with lysosomes to form autolysosomes.

Autophagy-related genes (ATGs) code for the proteins involved in formation and maturation of the autophagosome and its consequent fusion with the lysosome.[21] Several genetically modified mouse models have been used to investigate the cellular changes caused by defective autophagy in the nervous system.[13,17] Impaired autophagy has also been linked to spontaneously occurring neurological diseases in domestic animals.[1,12,18] We recently identified a missense change, c.1288G>A; p.Ala430Thr, in the cysteine proteinase gene *ATG4D*, associated to a progressive neurological disease in Lagotto Romagnolo dogs (LRs).[18] *ATG4D* cleaves microtubule-associated protein 1A/B light chain3 (LC3), enabling its lipidation into LC3-II and consequent incorporation in the autophagosomal membrane. LC3 is a widely used marker for this compartment. *ATG4D* also delipidates LC3-II from the autolysosomal membrane,[8] providing a cytoplasmic pool of free unlipidated LC3-I, which can be reused. Regardless of the increasing evidence for cross-talk between autophagy, endo-lysosomal sorting, and nonconventional secretion, few spontaneous diseases due to alterations in these functions have been described. The affected LRs show an extensive histopathological extraneural phenotype characterized by severe cytoplasmic vacuolization of various cells. The aim of this study was to test the hypothesis that autophagy is altered in affected dogs, to further investigate the histopathology of extraneural target tissues and to screen for known lysosomal storage diseases with overlapping findings in the affected dogs.

Materials and Methods

Animals

Tissues from 9 privately owned LR dogs with progressive cerebellovestibular dysfunction associated with the *ATG4D*$^{mut/mut}$ genotype (c.1288G>A; p.Ala430Thr) were included in the study. Two dogs underwent postmortem examination at the University of Veterinary Medicine Hannover, Germany (dog Nos. 6 and 7); 1 each at the University of Bern, Switzerland (dog No. 5); the Clinica Neurologica Veterinaria in Milano, Italy (dog No. 9); the Norwegian University of Life Sciences, Oslo, Norway (dog No. 8); and 4 at the University of Helsinki, Finland (dog Nos. 1–4). Four additional LRs with the same genotype, regardless of clinical signs, were prospectively recruited for skin biopsy (dog Nos. 10–13). Tissue samples from 4 *ATG4D*$^{wt/wt}$ LR dogs euthanized for unrelated reasons were used as control material. Demographic data on the affected and control dogs included in the study are presented in Table 1.

Ethics Statement

Euthanized affected and control dogs were privately owned pets, euthanized and autopsied at the owners' request due to progressive clinical signs. Skin biopsies were obtained with the owners' consent and according to clinical standards approved by the Animal Ethics Committee at the State Provincial Office of Southern Finland (permit: ESAVI/6054/04.10.03/2012).

Cell Culture and Starvation Experiments

Fibroblasts from 2 affected dogs (dog Nos. 8 and 10) and 2 age-, breed-, and sex-matched controls (control dog Nos. 3 and 4) were cultured in high glucose Dulbecco's Modified Eagle Medium (DMEM 41965-039 Gibco) with 10% fetal bovine serum (FBS 10500056 Gibco) and penicillin-streptomycin

Table 1. Demographic Data Regarding the Lagotto Romagnolo Dogs Included in the Study.

Autopsy Case No.	Country of Origin	Sex	Age at Euthanasia	Age at Onset of Signs	Disease Duration (mo)
1	FI	M	2 y 5 mo	1 y 7 mo	10
2	FI	M	2 y 4 mo	1 y 1 mo	15
3	FI	F	1 y 8 mo	4 mo	16
4	FI	F	8 y	4 y	48
5	CH	F	2 y 9 mo	2 y 6 mo	3
6	SE	M	2 y	1 y 9 mo	3
7	SE	M	6 y 8 mo	1 y 6 mo	64
8	NO	F	4 y	1 y 7 mo	31
9	ITA	M	8 y	not specified	not specified
Biopsy Case No.	**Country of Origin**	**Sex**	**Age at Sampling**	**Age at Onset of Signs**	**Disease Duration (m)**
10	FI	F	5 y	3 y	29
11	FR	F	8 y	No signs	n/a
12	FI	F	5 y	3 y 3 mo	26
13	USA	F	2 y	1 y 6 mo	13
Control Case No.	**Country of origin**	**Sex**	**Age at Sampling**	**Disease**	
1	FI	F	8y	Idiopathic epilepsy	
2	FI	M	5y	Hemangiosarcoma	
3	FI	F	4y	Mammary tumor	
4	FI	F	5y	Skin tumor	

Abbreviations: CH, Switzerland; FI, Finland; FR, France; ITA, Italy; NO, Norway; SE, Sweden; USA, United States of America.

(PenStrep15140122 Gibco). During second or third passages, cells were seeded at equal density onto Petri dishes and additionally onto glass cover slips. At semi-confluency, the cells were incubated in fresh medium for 2 hours, with and without 0.4 μM bafilomycin (Bafilomycin $_{A1}$ BioViotica NSC381866), or subjected to a 2-hour starvation in Earl's Balanced Salt Solution (EBSS 24010043Gibco) with and without 0.4 μM bafilomycin. The cells were harvested and lysed with RIPA buffer containing 0.5 M Tris-HCl, pH 7.4, 1.5 M NaCl, 2.5% deoxycholic acid, 10% NP-40, 10 mM EDTA (R0278 Sigma), and an EDTA-free protease inhibitor cocktail (SigmaFAST S8830). The lysates were subjected to Western blotting (WB) with anti-LC3 antibody (anti-LC3 L7543 Sigma-Aldrich). Beta actin was used as the loading control for relative quantification of the blots (anti-beta Actin PA5-16914 Thermo Fischer Scientific). Signals were visualized by enhanced chemiluminescence. The blotting experiments were conducted as 2 technical replicates of the 2 affected and 2 age-, gender-, and breed-matched controls. Results were evaluated for significant differences using the two-tailed *t*-test for independent samples.

Immunofluorescence

Fibroblasts were fixed with methanol at –20°C for 5 minutes onto coverslips under basal conditions, with and without 0.4 μM bafilomycin, and after a 2-hour starvation in EBSS. The coverslips were stained for immunofluorescence with primary antibodies against LC3 (Abcam ab48394) and LAMP2 (LSBio 3144) and secondary antibodies conjugated to Alexa Fluor 594 (A11037 Thermo Fisher) for LC3 and Alexa Fluor 488 (A11029 Thermo Fischer) for LAMP2. Four, 5-diamidina-2-phenylindole (62248 DAPI Solution 1 mg/mL Thermo Fisher) was used to envision the nuclei. The coverslips were mounted onto microscopy slides and viewed under a Zeiss Axio Imager A2 fluorescence microscope. The emission was captured with a Zeiss AxioCam MRc5, set at 90% exposure intensity for 40 milliseconds. The number of LC3-positive spots in 50 cells at 0 hours, with and without 0.4 μM bafilomycin, and at 2-hour starvation was analyzed with Cell Profiler software.[4] The results were tested for significance as age-matched pairs with the Mann-Whitney *U*-test and between the 4 dogs using the Kruskall-Wallis test.

Histopathological Examination

Autopsy was performed in 8 LR dogs (dog Nos. 1–8). Samples of the major internal organs, skin, central nervous system (CNS), and peripheral nerves were formalin fixed, paraffin embedded, and processed for routine histology. The brain and a skin biopsy were formalin fixed and examined from the ninth euthanized dog (dog No. 9). Skin biopsies from the dorsal flank area of 4 additional living LRs were formalin fixed, paraffin embedded, and processed for routine histology. Tissue sections of the formalin-fixed material were stained with hematoxylin-eosin (HE), periodic acid-Schiff (PAS), and PAS-diastase. Fresh-frozen tissue samples were prepared from the pancreas and skin of 2 affected (dog Nos. 2 and 3) and 1 control dog (control dog No. 1) and stained with PAS and Oil-red-O for glycoproteins and lipids, respectively. Antibodies used for immunohistochemical staining included anti-p62/sequestosome 1 as marker for autophagic cargo (Sigma-Aldrich P0067), anti-LC3A/B for autophagosomal membranes (LC3B; Abcam ab48394), and anti-LAMP2 for the integral membrane protein

of late endosomes, lysosomes, autolysosomes, and secretory lysosomes (LAMP2; LSBio 3144). The antigens were retrieved with 0.01 M citrate buffer at pH 6 and heated for 20 minutes at 99°C. The sections were stained according to the UltraVision Detection System HRP/DAB kit (Thermo Fisher Scientific Inc.). Electron microscopy (EM) samples from the pancreas and mandibular salivary gland of 2 affected dogs (dog Nos. 2 and 8), skin of 3 affected dogs (dog Nos. 2, 8, and 10), and respective tissues from 1 control dog (control dog No. 1) were fixed in 2.5% glutaraldehyde, postfixed with 1% osmium tetroxide, stained with 8% uranyl acetate in 0.69% maleic acid, and embedded in epoxy resin. Ultrathin sections were mounted on copper grids, stained with Reynolds lead citrate, and viewed with a Jeol JEM-1400 (Jeol Ltd., Tokyo, Japan) electron microscope equipped with a Gatan Orius SC 1000B bottom mounted CCD-camera (Gatan Inc., USA) at 80 KV.

Biochemical Screening for Stored Material and Lysosomal Enzyme Activity

Urine samples of 2 affected dogs (dog Nos. 1 and 10) were analyzed by thin-layer chromatography and stained with resorcinol to identify the excreted oligosaccharides. Samples of 2 clinically healthy dogs were included as canine controls. Laboratory control samples of a healthy human and a human with Salla disease were included as negative and positive controls for the staining. The glycosaminoglycan (GAG) concentration was measured based on the color reaction with dimethylmethylene blue as described by de Jong et al,[5] and the ratio of urinary GAG to urinary creatinine was counted to compensate for the concentration differences in the native urine samples. Fibroblasts from the skin biopsies of 3 affected dogs (dog Nos. 8, 10, and 12) and 2 controls (dog Nos. 3 and 4) were cultured, and the enzyme activity levels of beta-galactosidase (b-Gal), arylsulfatase A (ARYLS-A), and glycosylasparaginase (GA) were measured. The GA activity was also determined in the culture medium of the affected and control cells. The formation of 4-methylumbelliferone from the substrate of 4-methylumbelliferyl-beta-D-galactoside by b-Gal, of p-nitrocatechol from p-nitrocatechol sulfate by ARYLS-A, and 7-amido-4-methylcoumarin from L-aspartic acid β-7-amido-4-methylcoumarin by GA was followed by a kinetic measurement, using microtiter plate spectrofluorometry (b-Gal, GA) or spectrophotometry (ARYLS-A). The enzyme activity was expressed as nanomoles of substrate hydrolyzed per minute per mg protein in the sample preparation.

Results

Basal Autophagy Is Altered in Fibroblasts With the ATG4D Variant

Cytosolic LC3-I and membrane-bound LC3-II can be separated by WB as approximately 16 kDa and 18 kDa bands, respectively. The LC3-II level has been shown to correlate with the amount of autophagosomes[25]. Under basal conditions, LC3-II levels were higher in the affected cells when compared with the control cells (Fig. 1A). The difference in LC3-II levels under basal conditions was statistically significant when quantified against the sample's beta actin load (Fig. 1B). Multiple bands of beta-actin were noted in all lanes, with less than 1 kDa molecular weight difference. The total intensity of the multiple beta-actin bands was used when quantifying the gel as the bands may represent post-translationally modified beta-actin detected by the polyclonal antibody. When lysosomal degradation was blocked with bafilomycin under basal conditions, LC3-II levels increased in both affected and control cells as expected. However, the increase in LC3-II in affected cells was milder, and the difference between control and affected cells was no longer statistically significant, indicating that lysosomal degradation of autophagic cargo is less effective in cells with the ATG4D variant. Under starvation conditions, the levels of LC3-II remained comparable between the control and the affected cells (Fig. 1B), and a similar increase in LC3-II was noted in both samples after lysosomal inhibition with bafilomycin (Fig. 1A, B). These findings suggest that basal autophagy but not starvation-induced autophagy is altered in the

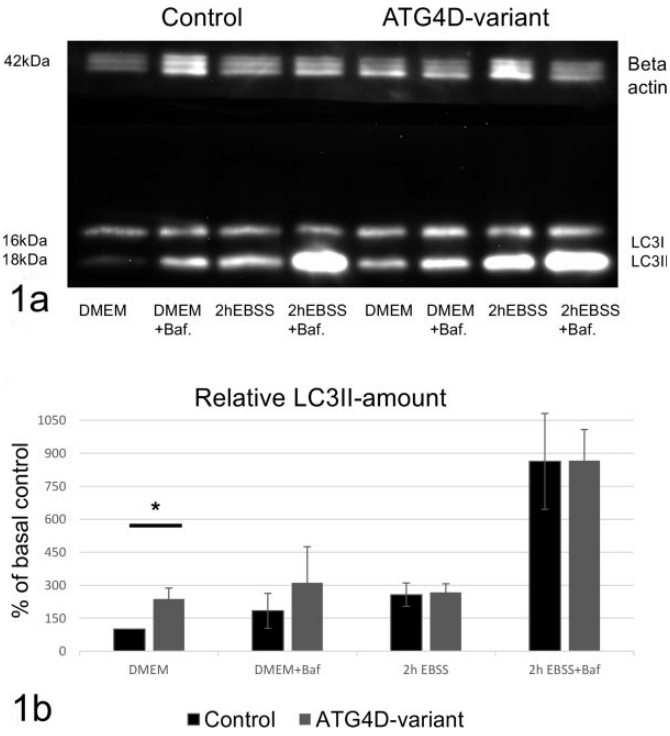

Figure 1. Western blot analysis of LC3 levels in fibroblasts from affected and control dogs. **(a)** Western blot of lysates from fibroblasts of control and affected dogs under basal conditions in Dulbecco Modified Eagle Medium (DMEM) and starvation conditions in Earl's Balanced Salt Solution (EBSS), with and without lysosomal inhibitor bafilomycin (Baf.). The *ATG4D* variant shows a LC3-II band at basal conditions (*ATG4D*, DMEM) in contrast to control (Control, DMEM). **(b)** LC3-II levels were quantified against beta actin in 2 affected and 2 control dogs, and a significantly higher level of LC3-II was noted in the *ATG4D* variant at basal conditions (DMEM). Results are shown as %, with the mean LC3-II level of controls in DMEM set as 100%. Columns and error bars represent the mean and SD of 4 experiments. *$P < .005$.

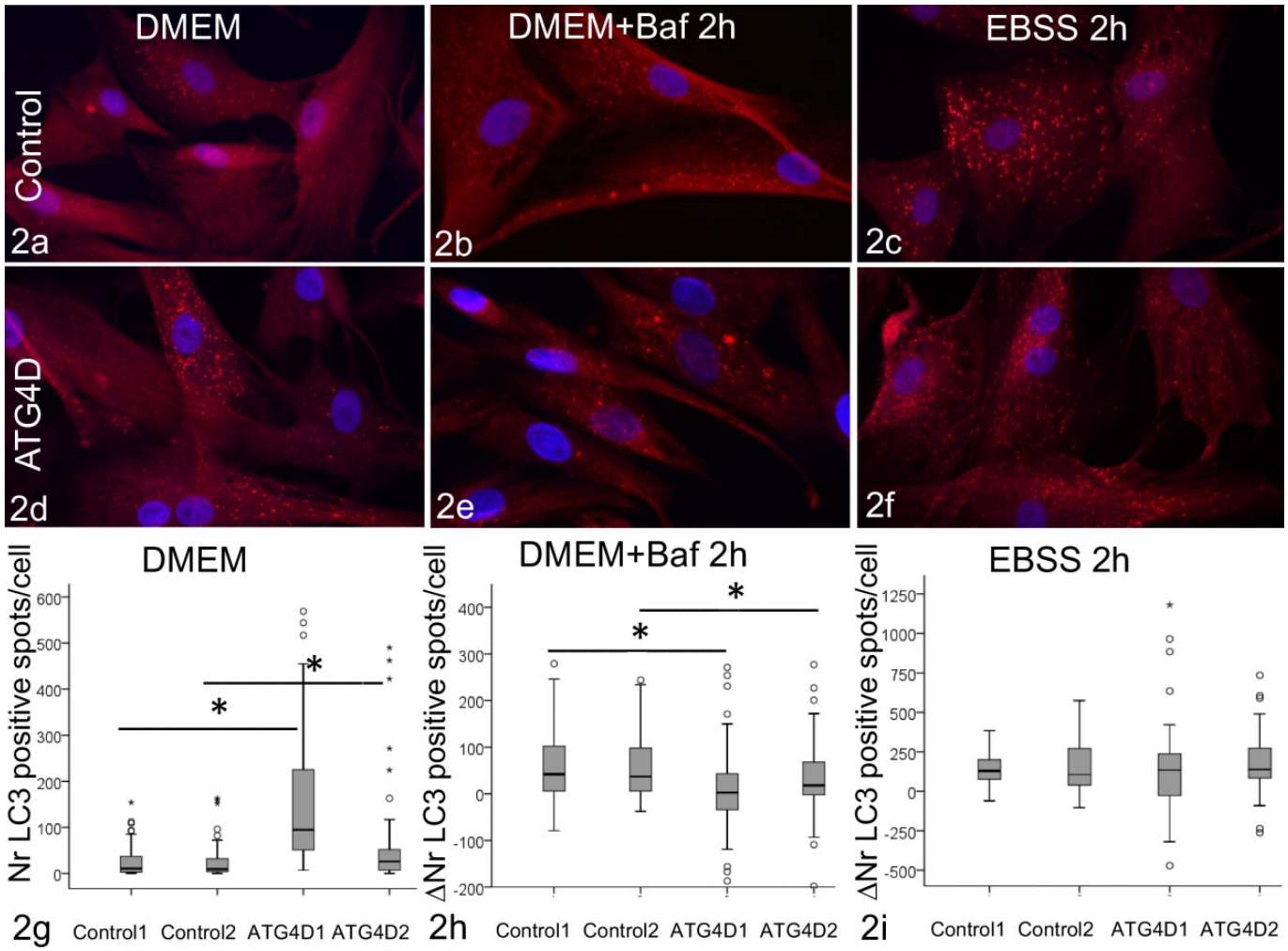

Figure 2. LC3 immunofluorescence in canine fibroblasts from affected and control dogs. **(a–f)** LC3 is shown in red and the nuclei in blue. The left column represents affected (bottom, ATG4D) and control (top) cells under nutrient-rich conditions. The middle column shows affected (bottom) and control (top) cells subjected to a lysosomal inhibitor under nutrient-rich conditions. The right column represents affected (bottom) and control (top) cells under starvation. A gradual increase in number of red spots, corresponding to autophagosomes, is seen from left to right in controls. Affected cells contain numerous positive spots already during basal conditions. Boxplots of the **(g)** number and **(h, i)** increase of LC3-positive spots in 50 cells at full culture medium (DMEM), full culture medium with bafilomycin (DMEM+Baf.), and in starvation medium (EBSS) $^*P < .05$. Affected cells (ATG4D) have significantly more LC3 labeled spots (autophagosomes) at basal state when compared to controls, indicating that basal autophagy is altered in affected animals. There is also a significant difference in the increase in number of autophagosomes between affected and control cells when lysosomal degradation is inhibited under basal conditions. No significant differences are noted in the increase in number of spots when autophagy is induced, indicating that starvation-induced autophagy is as efficient in affected as in control cells.

ATG4D variant cells. Further, since bafilomycin caused a milder increase in LC3-II levels in affected cells under basal conditions, it is likely that the LC3-II accumulation observed in these cells during basal autophagy is in part due to decreased lysosomal degradation of autophagic cargo.

Immunofluorescence staining was used to visualize autophagosomes as LC3-positive cytoplasmic spots. In agreement with the WB results, the median number of LC3-positive spots under basal conditions was significantly higher in the affected cells than in the controls cells (Fig. 2A, D, G). When lysosomal degradation was inhibited by bafilomycin in nutrient-rich conditions, the increase in number of spots was significantly milder in affected when compared to control cells (Fig. 2H). The total number of LC3-positive spots was comparable between affected and controls (Fig. 2B, E). As expected, starvation increased the number of spots regardless of the ATG4D-status of the cells (Fig. 2C, F), and the increase in the number of LC3 spots after the 2-hour starvation was not significantly different in the affected cells (Fig. 2I). The absolute number of LC3-positive spots was higher in affected cells than in control cells after 2-hour starvation, reflecting the higher basal level at start. The high number of LC3-positive puncta despite a comparable LC3-II/vimentin ratio in the affected cells during induced autophagy may indicate that LC3-II is present in lower

density on more numerous vesicles in the affected cells. To conclude, both WB and immunofluorescence results suggest that basal but not induced autophagy is altered in the affected cells. Since inhibiting lysosomal degradation with bafilomycin induced a milder increase in LC3-II level and number of spots in affected cells than in controls, it is likely that lysosomal degradation is decreased in affected cells under basal conditions. This can be due to impaired fusion of autophagosomes with lysosomes, impaired capacity of lysosomes to degrade the cargo, or both.

Cytoplasmic Vacuolization Affects Cells Active in Secretion and/or Transcytosis

We recently showed that LRs with the *ATG4D* variant have neuropathological changes, such as spheroids, with ultrastructural and immunohistochemistry (IHC) findings compatible with altered autophagy.[18] However, the cytoplasmic vacuolization noted in neurons as well as specific extraneural tissues has not previously been linked to changes in autophagy. In this study, we investigated the ultrastructure of affected extraneural target tissue, namely, tissues active in secretion and/or transcytosis. Extensive diffuse cytoplasmic vesiculation with cellular hypertrophy was present in the dermal apocrine glands of living affected dogs in 3 of the 4 examined skin biopsies and in all autopsied dogs (Fig. 3). Similar changes affected the pancreatic acinar cells, the acini and secretory ducts of the serous salivary glands, mammary glands, and the apocrine glands of the anal sac. Cells involved in secretion and transcytosis in the eye and ear, including the epithelial cells of the lacrimal gland, the ciliary body, lenticular epithelium, corneal endothelium, and the marginal cells of the otic stria vascularis, were also vacuolated. Numerous small, less evident cytoplasmic vesicles were present in the thyroid follicular cells, adrenal cortical cells, renal distal convoluted tubules, and hepatocytes. In the mucous salivary glands and the parathyroid gland, the cells appeared hypertrophic with cytoplasmic clearing in HE staining but without distinct cytoplasmic vesiculation as seen in the serous secretory cells. Selected mesenchymal cells were also affected by the disease. Small pre- and postcapillary vessels in the CNS, heart, skin, renal glomeruli, ganglia, and glands, especially the pancreas, thyroid gland, and salivary glands, were prominent due to severe clear vacuolization of the cells of the tunica media. In PAS-staining, the vacuolar periendothelial cells were enwrapped by the basement membrane, indicating that they represented pericytes (Fig. 4). The renal capillary loops and distal convoluted tubules were affected by vacuolization (Fig. 5). The cytoplasm of the pulmonary alveolar macrophages was vesicular, and in the peripheral lymph nodes, the plasma cells (Fig. 6) and macrophages contained large clear cytoplasmic vacuoles. The vacuolar content did not stain with PAS or lipid stains. The smooth muscle cells of the urinary bladder, gastrointestinal wall, and skin contained multifocal, granular, cytoplasmic, and eosinophilic PAS-positive material. LAMP2-positive membranous staining was present in the vacuoles of the acinar cells in the sweat glands (Fig. 7), in contrast to the punctate staining in the controls (inset Fig. 7). Partial membranous immuno-labeling for LAMP2 was noted in the macrophages of both affected and control dogs, whereas LAMP2, LC3B, and p62 immunoreactivity were absent in other vacuolated cells. The granular material within the smooth muscle cells stained positively for both p62 (Fig. 8) and LC3B.

MVB and Single Membrane–Bound Vacuoles Accumulate in Affected Cells

Electron microscopic examination of the sweat glands showed numerous single membrane–bound vacuoles, up to 1 μm in diameter, within the cytoplasm (Fig. 9). The vacuolar content was sparse, with some vacuoles appearing empty. Occasional engulfment and fusion between vacuoles was also seen (Figs. 9, 10 arrows), and some vacuoles showed inverted budding of vesicles (Fig. 10 short arrow). In the acinar cells of the pancreas and serous salivary glands, the light microscopical change corresponded with multiple single membrane–bound, basal vacuoles, ranging from 1 to 5 μm in size (Fig. 11). Fusion among the clear vacuoles (arrow) and between the clear vacuoles and late autophagic vacuoles (asterix) was occasionally noted in the affected acinar cells (Fig. 12). Specific secretory granules were present in the apical part of the affected cells. Basally in the cells, few autophagic vacuoles containing remnants of zymogen granules were seen in both the affected and control pancreas. EM of the small vessels of the pancreas revealed cytoplasmic vacuoles in the smooth muscle cells and pericytes as single membrane–bound empty spaces exceeding the size of the nucleus (Fig. 13). Numerous small, membrane-bound vesicles approximately 500 nm in diameter, with variable content and evenly distributed throughout the cell, were present within the endothelial cells (Fig. 14).

Biochemical Screening and Cell Assays Did Not Indicate a Lysosomal Storage Disease

The light microscopic findings in the affected dogs bear resemblance to lysosomal storage diseases. Considering the close link between autophagy and lysosomal degradation, biochemical screening methods were used to study whether the affected dogs suffer from a known lysosomal storage disease. The pattern of excreted oligosaccharides in the urine, staining brown in resorcinol staining, was comparable between the affected and control dogs (Supplemental Figure S1). Increased excretion of free sialic acid, staining blue in resorcinol staining, was not present in the urine of affected dogs when compared with the canine controls and the Salla disease laboratory control sample. The amount of GAGs in the urine of affected dogs was lower than or similar to that of the controls (Table 2), and the maximum urinary GAG/Crea ratio in the tested affected dogs was 3.1, when the mean U-GAG/ U-Crea ratio in human mucopolysaccharidoses is 512 (SD = 266.6, $n = 33$).[10]

A several-fold difference in enzyme activity levels of specific lysosomal enzymes (decrease intracellularly or increase

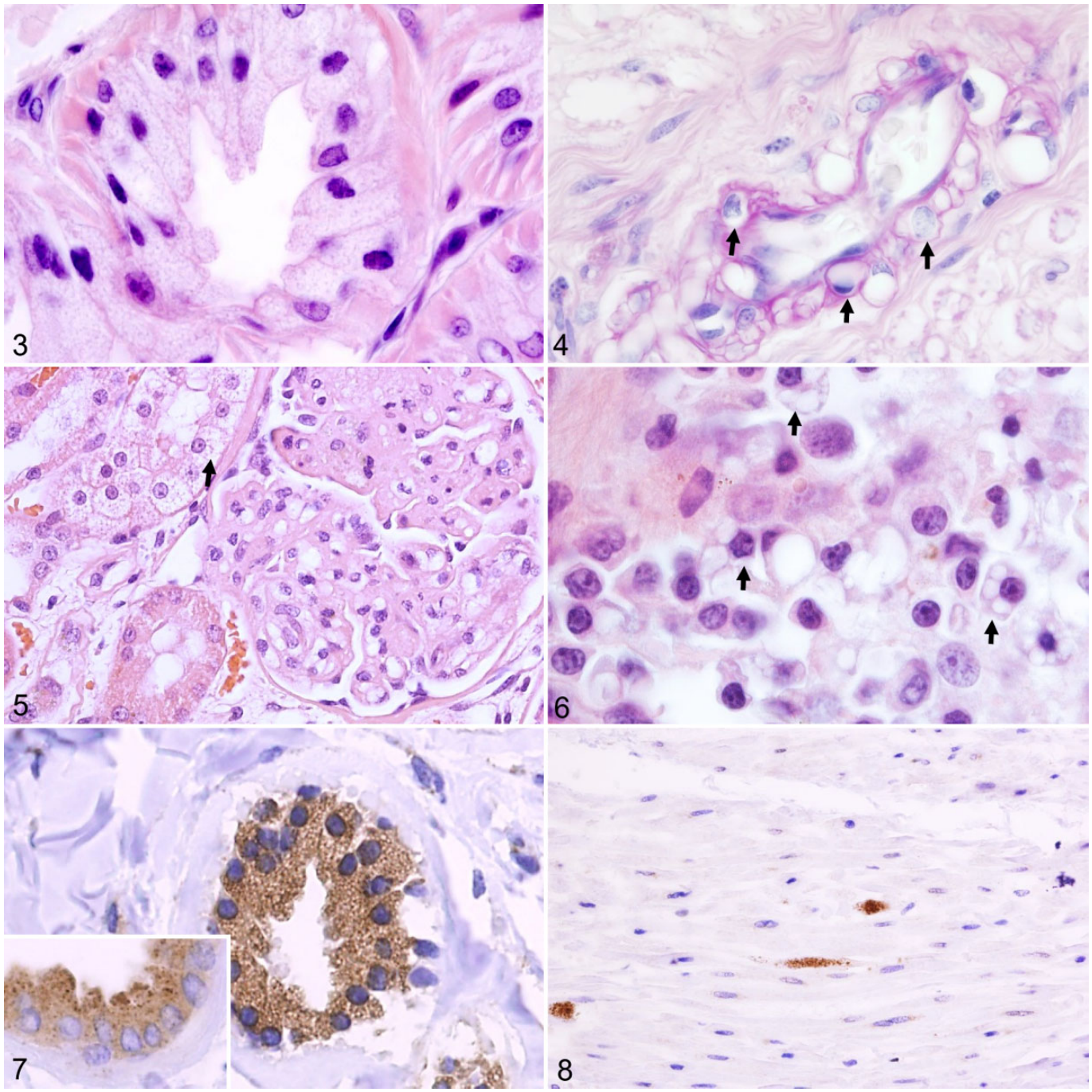

Figures 3–8. Autophagy-related vacuolar disease, Cytoplasmic vacuolization of extraneural affected organs, dog, *ATG4D*$^{mut/mut}$. **Figure 3.** Apocrine sweat glands of the skin show extensive cytoplasmic vesiculation. HE. **Figure 4.** Tunica media of numerous small pre- and postcapillary vessels is highly vacuolated. Basal membranes line the vacuolated cells (arrows), which is typical for pericytes. Periodic acid-Schiff. **Figure 5.** Podocytes and endothelial cells within the renal glomerula are highly vacuolated, as are the epithelial cells of the distal convoluted tubules (arrow). HE. **Figure 6**. Plasma cells (arrows) within the lymph nodes show large distending clear vacuoles within the cytoplasm. HE. **Figure 7.** Apocrine sweat gland: the vesiculation of the apocrine sweat glands in the skin is strongly LAMP2 positive. In the controls, punctate lysosomal staining is present (inset). IHC for LAMP2. **Figure 8.** Smooth muscle cells contain granular p62-positive intracytoplasmic material. IHC for p62.

extracellularly) are characteristic of lysosomal storage diseases.[29,33] We measured the activity of the selected lysosomal hydrolases in cultured fibroblasts and the activity of glucosylasparaginase in the culture medium (Table 3). The mean intracellular enzyme activity level of all measured enzymes was slightly increased in the affected cells in comparison to controls. Standard deviations were, however, partially overlapping, and several-fold differences between

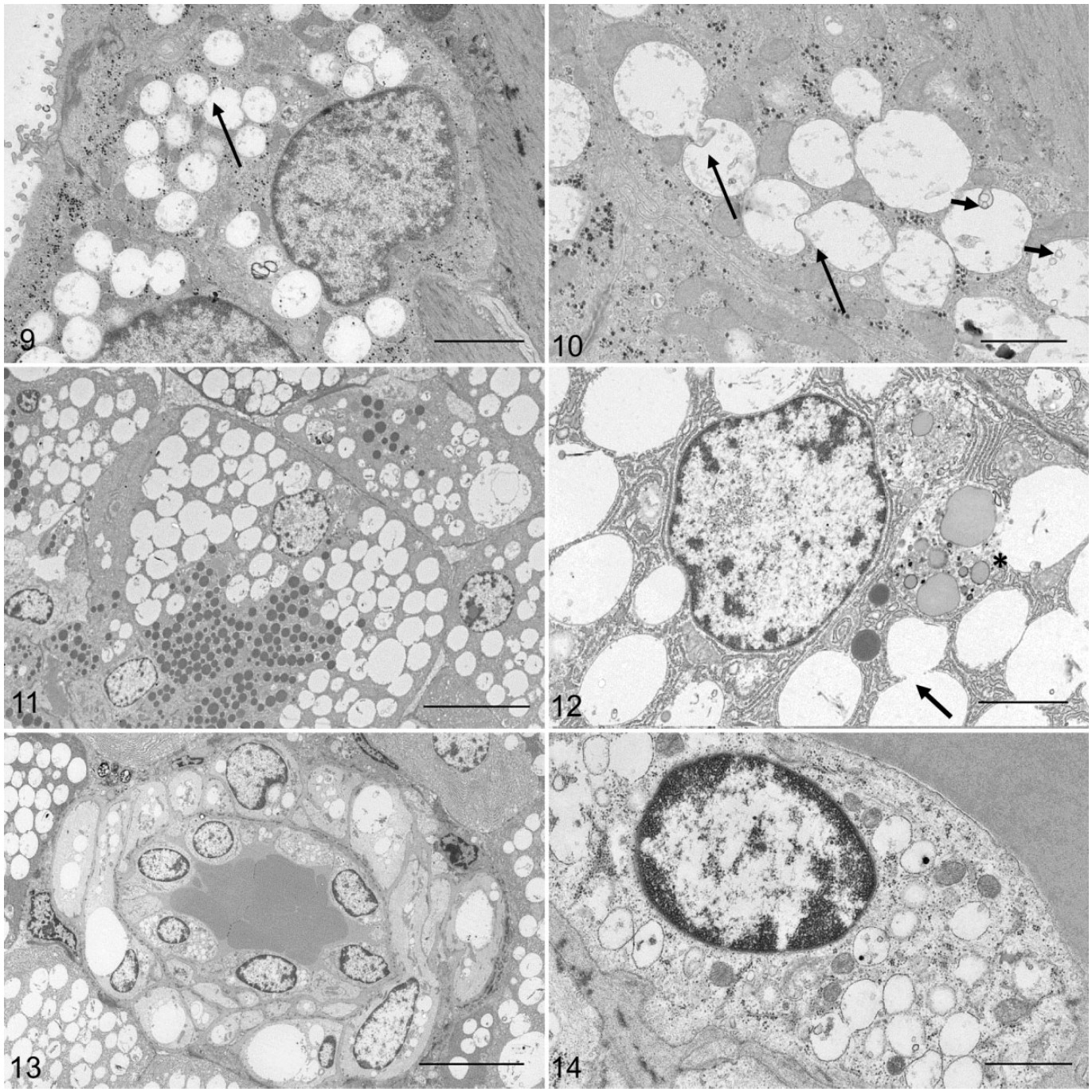

Figures 9–14. Autophagy-related vacuolar disease, dog, *ATG4D*$^{mut/mut}$. **Figure 9.** Sweat gland, acinar cells: Single membrane–bound vesicles, uniform in size, are distributed throughout the cytoplasm and fuse with each other (arrow). Bar 2 μm. **Figure 10.** Sweat gland, acinar cell: The vacuolar content is sparse, with inverted budding (short arrows) and engulfment (long arrows) between the vacuoles. Bar 1 μm. **Figure 11.** Pancreatic acinar cell: The pancreatic vacuolization is more variable in size, with the largest vacuoles being up to 5 μm in diameter. Bar 10 μm. **Figure 12.** Pancreatic acinar cell: The vacuoles fuse with each other (arrow) and with autophagic vacuoles (asterisk). Bar 2 μm. **Figure 13.** Vessel: Perivascular mesenchymal cells embedded in the basal lamina, consistent with pericytes, contain large single membrane–bound vacuoles in the cytoplasm. Bar 10 μm. **Figure 14.** Endothelial cell: Vacuolization of the cytoplasm is evident also in the endothelial cells that contain small vesicles, approximately 0.5 μm in size, evenly distributed throughout the cell. Bar 1 μm.

affected and controls in the measured levels were not detected. The extracellular enzyme activity was overlapping or slightly lower in affected samples compared to controls. The results suggest that lysosomal degradation is not markedly altered in the affected cells. This conclusion in supported by the finding that LC3-II levels further increased during starvation when the lysosomal inhibitor bafilomycin A_1 was present in the medium (Fig. 1B). This indicates that

Table 2. Urinalysis of Excreted Amount of Glycosaminoglycans in 2 Affected Dogs and 2 Control Dogs.

Case No.	U-GAG mg/l	U-Crea mmol/l	U-GAG/ U-Crea[a]	Age
Affected dog No. 1	8.8	2.8	3.1	2 y
Affected dog No. 10	24.9	16.3	1.5	5 y
Control	23.7	15.2	1.6	2 y
Control	34.6	13.8	2.5	7 y

Abbreviations: U-Crea, urinary creatinine; U-GAG, urinary glycosaminoglycans.
[a]The U-GAG/Crea ratio is used to compensate for concentration differences between the native urine samples of the animals.

lysosomal degradation was functional in the affected fibroblasts at least under starvation conditions.

Discussion

In this study, we report an altered basal autophagy with a vacuolar cytoplasmic and ultrastructural change in a naturally occurring canine disease. When monitored by WB and immunofluorescence, fibroblasts from LRs with a missense variant in the *ATG4D* had significantly higher LC3-II levels and a higher amount of LC3-positive spots under nutrient-rich conditions than did the controls. However, the difference disappeared during starvation-induced autophagy. There are 2 known causes for increased LC3-II levels in cells: increased formation of autophagosomes or blocked autophagic flux with decreased autophagosome-lysosome fusion or autophagic degradation.[24] These 2 can be differentiated by the use of lysosomal inhibitors, which cause an increase in LC3-II levels if the cells have a functional lysosomal degradation. When adding a lysosomal inhibitor during basal autophagy, we observed a milder increase in LC3-II levels and number of LC3-positive spots in affected cells than in controls. This indicates that autophagic flux is decreased in the affected cells under basal conditions. As the differences in LC3 disappeared during starvation and we found no further evidence of a lysosomal storage disease, it is likely that the decreased basal autophagic flux is due to impaired fusion of autophagosomes with lysosomes and not disturbed lysosomal degradation. Autophagy induction is expected to present as increased numbers of double-membraned autophagosomes, and this was not observed in the affected dogs. Instead, the ultrastructural findings in affected canine tissues indicate vesicular accumulation. The cytoplasmic vacuoles in the affected LRs showed ultrastructural features reminiscent of enlarged endosomes or MVBs, with internal budding and vesiculation. Another possibility is that the vacuoles represent amphisomes as some single membrane–bound, LAMP2-negative vacuoles were observed to fuse with autophagic vacuoles. This suggests involvement of the endosomal pathways in the vacuole formation in this disease.

Our results suggest that basal but not induced autophagy is altered in the affected cells. Interestingly, an association between basal autophagy and late endosomal function was recently revealed in detail.[26] Murrow and colleagues[26] described altered basal autophagy with increased numbers of LC3-positive puncta in cells with disrupted ATG12-ATG3 conjugation. They further demonstrated defective endo-lysosomal traffic and accumulation of perinuclear MVBs and late endosomes in the cells, thereby linking the core autophagy and the endosomal sorting complexes required for transport. Starvation-induced autophagy was effective in the cells despite the disturbed basal autophagy.[26] A recent study also showed that the clearance of autophagic vacuoles is indeed regulated differently under basal and starvation conditions.[34]

We report here a prominent accumulation of vesicles in several cell types of the affected dogs. Previously, a similar ultrastructural change was described in differentiating human erythroblasts, in which autophagy is responsible for organelle clearance.[2] Expression of a dominant negative *ATG4D* mutant led to retention of expanding amphisomes in the maturing cells.[2] Interestingly, the retention of amphisomes did not markedly alter the differentiation of erythroid cells; thus, autophagy completed its function despite the ultrastructural change. Likewise, signs of markedly disturbed functioning of the affected extraneural organs in the LRs were not detected during the clinical examination, necropsy, or routine histology. The sole clinical complaint in the dogs was neurological signs, corresponding to lesions in the axons and Purkinje cells,[18] structures known to be dependent on basal autophagy.[13]

Tethering, hemifusion, and true fusion were other features of the cytoplasmic vacuoles observed in the LRs. LC3-II has an intrinsic capacity for polymerization and tethering within membranes in several mammalian cell types.[9] The *ATG4*-mediated delipidation of LC3-II provides a pool of free LC3-I for de novo autophagosome assembly in yeast and prevents erroneous accumulation of LC3-II on organelles such as the endosome.[27] Excessive LC3-II and possibly erroneous deposition of LC3-II on endosomal membranes are possible causes for the aggregating vesicles in the affected dogs.

The cytoplasmic vacuolization was present in cells that are active in secretion, especially in epithelial cells with conventional serous secretion. Autophagy plays a specific role in these cells by digesting excess secretory granules in a form selective autophagy, referred to as crinophagy.[11,31] Thereby, the secretory granules are enclosed in the autophagosome and delivered to the lysosome for digestion. However, neither the EM findings nor the IHC indicated a disturbance in this function in the affected LRs. No accumulation of secretory granules in the salivary or pancreatic acinar cells was seen, and the vacuolization of the acinar cells was LC3B negative and the vacuoles single membrane–bound. Further studies are needed to determine the exact origin and nature of the vacuoles. The changes in the sweat glands, however, differed from the findings in other serous secretory cells since the vacuolar membranes were LAMP2 positive. LAMP2 is an integral membrane protein in several compartments, including late endosomes, autolysosomes, secretory lysosomes, and conventional lysosomes.[3] Direct engulfment of cytoplasmic fragments by late endosomes

Table 3. Activity of Lysosomal Enzymes in Fibroblasts and Growth Medium.

Case No.	Beta-galactosidase (nmol/min/mg)	Arylsulfatase-A (nmol/min/mg)	Glycosyl-asparaginase cells (pmol/min/mg)	Glycosyl asparaginase medium (pmol/min/mg)
8	14	1	59	30
10	6	1	n/a	25
12	24	8	109	49
Mean, SD	14.7 ± 7.1	3.3 ± 5	84 ± 35.4	34.7 ± 13.4
Controls				
Dog No. 1	10	2	99	53
Dog No. 3	6	1	n/a	38
Mean, SD	8 ± 2.8	1.5 ± 0.7	49.5 ± 70	45.5 ± 10.6

or lysosomes, as seen in the sweat glands of the dogs, is the morphological correlate of microautophagy.[20] In contrast to the conventional secretion in the other affected glands, apocrine secretion in canine sweat glands occurs through direct blebbing of the apical cytoplasm without involvement of the endoplasmic reticulum, Golgi, and secretory granules. Whether this difference in secretory mechanisms underlies the differences in ultrastructural changes between the various glands was not further investigated. Alternatively, microautophagy in the apocrine sweat glands could be a compensatory attempt for altered basal autophagy because the 3 forms of autophagy are complementary to each other.[20,24]

The mesenchymal cells affected by vacuolization in the affected LRs all have in common a high rate of intracytoplasmic vesicular movement, and specific roles for autophagy have been described in many of the target cells. Glomerular podocytes are post-mitotic pericyte-derived cells that specialize in transcytosis and show exceptionally high levels of basal autophagy for glomerular maintenance.[14] In both macrophages and vascular endothelial cells, autophagic membranes participate in unconventional secretion of vesicles, and interestingly, *ATG4D* was detected in the secretome of endothelial cells.[6,30] Endothelial deletion or knock-down of *ATG5* or *ATG7* lead to changes in unconventional secretion of von Willebrand factor but not to altered vessel architecture or density.[32] Furthermore, functional autophagy is necessary for sustainable antibody production in plasma cells, which show a significantly higher autophagic flux than the naive B-cells.[28]

The light microscopic findings in the affected dogs bear resemblance to lysosomal storage diseases. Therefore, exclusion of known lysosomal storage diseases with similar target organs, biochemical and ultrastructural properties of the storage, was indicated in the affected dogs. Basic screening methods for lysosomal storage disease revealed neither differences in urinary oligosaccharide and GAG excretion nor changes in lysosomal enzyme activities in comparison to control dogs. The maximum urinary GAG/Crea ratio in the tested affected dogs was 3.1, while the mean U-GAG/ U-Crea ratio is 512 (SD = 266.6) in humans ($n = 33$) affected by various forms of mucopolysaccharidoses.[10] A several-fold difference in enzyme activity levels of specific lysosomal enzymes (decrease intracellularly or increase extracellularly) are characteristic of lysosomal storage diseases.[29,33] The mean activity level in the intracellular enzymes measured in affected cells was in fact slightly higher than that of the corresponding controls. The maximum extracellular enzyme level did not exceed that of the controls. In addition, the LC3-II levels were similar in control and affected cells under starvation conditions, indicating that lysosomal degradation was functional at least under starvation. Finally, with one exception, we did not observe accumulation of LAMP2-positive lysosomal vesicles in the cells and tissues of the affected dogs. All these results support the conclusion that the affected dogs do not suffer from a lysosomal storage disease.

LR dogs suffer from several neurological diseases, including cerebellar cortical degeneration with primary Purkinje cell loss, granuloprival cerebellar cortical degeneration, and benign familial juvenile epilepsy.[15,16] The phenotype described here represents yet another differential diagnosis for progressive neurological dysfunction in this breed. The consistent extraneural histopathological findings in the autophagy-related disease, especially the changes in the parathyroid, subcommissural organ, and microvasculature, distinguish the diseases. The lesions in the sweat glands, detectable in skin biopsies of living dogs, verified the diagnosis in all but 1 case in this study. The negative biopsy originated from an adult dog tested homozygous for the *ATG4D* variant repetitively and with clinical signs similar to those in other affected dogs. It remains to be seen in the follow-up of this dog whether the result could have been related to a reduced penetrance of the disease in some individuals or to limited sensitivity of the skin biopsy due to differences in the distribution of skin lesions between animals.

Conclusions

LRs homozygous for a missense variant in the *ATG4D* gene exhibit vacuolar cytoplasmic changes and altered basal autophagy with increased amounts of LC3-II under basal conditions. Ultrastructural findings in the vacuolated cells and the target cell selection, comprising cells with high membrane turnover and/or intracellular endo-lysosomal traffic, suggest that the altered basal autophagy affects vesicular pathways in these cells. The effects of a lysosomal inhibitor seen in the LC3 assay of affected fibroblasts, as well as further diagnostics by EM, histochemical stains, and biochemical screening, did not reveal any known lysosomal storage diseases in these dogs.

Acknowledgements

We kindly thank Professor Martin Renlund at the Department of Pediatrics, Helsinki University Central Hospital for performing the urine analysis and the Electron Microscopy Unit of the Institute of Biotechnology, University of Helsinki for providing laboratory facilities. We gratefully acknowledge Professor Arild Espenes, Randi SØrby, and Gjermund Gunnes at the Norwegian University of Life Sciences in Oslo for enabling autopsy and sampling of the Norwegian dog, as well as Itä-Suomen Laboratoriokeskus ISLAB and their specialist MD Jarkko Romppanen for analyzing the lysosomal enzyme levels in the canine fibroblasts.

Declaration of Conflicting Interests

The author(s) declared no potential conflicts of interest with respect to the research, authorship, and/or publication of this article.

Funding

The author(s) received the following financial support for the research, authorship, and/or publication of this article: venska Kulturfonden (http://www.kulturfonden.fi/) and the Finnish Veterinary Foundation/Helvi Knuuttila (http://www.etts.fi/en.html) are gratefully acknowledged for supporting the study, especially the electron microscopy. The study was partly supported by grants to HL from the Academy of Finland, ERANET-NEURONC, the Jane and Aatos Erkko Foundation and the Sigrid Juselius Foundation.

References

1. Agler C, Nielsen DM, Urkasemsin G, et al. Canine hereditary ataxia in old English sheepdogs and Gordon setters is associated with a defect in the autophagy gene encoding RAB24. *PLoS Genet*. 2014;**10**(2):e100399.
2. Betin VMS, Singleton BK, Parsons S, et al. Autophagy facilitates organelle clearance during differentiation of human erythroblasts. *Autophagy*. 2013; **9**(6):881–893.
3. Blott E, Griffiths GM. Secretory lysosomes. *Nat Rev Mol Cell Biol*. 2002;**3**(2): 122–131.
4. Carpenter AE, Jones TR, Lamprecht MR, et al. CellProfiler: image analysis software for identifying and quantifying cell phenotypes. *Genome Biol*. 2006; **7**(10):R100.
5. de Jong JG, Wevers RA, Liebrand-van Sambeek R. Measuring urinary glycosaminoglycans in the presence of protein: an improved screening procedure for mucopolysaccharidoses based on dimethylmethylene blue. *Clin Chem*. 1992; **38**(6):803–807.
6. Dupont N, Jiang S, Pilli M, et al. Autophagy-based unconventional secretory pathway for extracellular delivery of IL-1β. *EMBO J*. 2011;**30**(23):4701–4711.
7. Fader CM, Colombo MI. Autophagy and multivesicular bodies: two closely related partners. *Cell Death Differ*. 2009;**16**(1):70–78.
8. Fernandez AF, Lopez-Otin C. The functional and pathologic relevance of autophagy proteases. *J Clin Invest*. 2015;**125**(1):33–41.
9. Florey O, Overholtzer M. Autophagy proteins in macroendocytic engulfment. *Trends Cell Biol*. 2012;**22**(7):374–380.
10. Gallegos-Arreola MP, Machorro-Lazo MV, Flores-Martínez SE, et al. Urinary glycosaminoglycan excretion in healthy subjects and in patients with mucopolysaccharidoses. *Arch Med Res*. 2000;**31**(5):505–510.
11. Grasso D, Ropolo A, Lo Ré A, et al. Zymophagy, a novel selective autophagy pathway mediated by VMP1-USP9x-p62, prevents pancreatic cell death. *J Biol Chem*. 2011;**286**(10):8308–8324.
12. Hahn K, Rohdin C, Jagannathan V, et al. TECPR2 associated neuroaxonal dystrophy in Spanish water dogs. *PLoS One*. 2015;**10**(11):e0141824.
13. Hara T, Nakamura K, Matsui M, et al. Suppression of basal autophagy in neural cells causes neurodegenerative disease in mice. *Nature*. 2006;15;**441**(7095): 885–889.
14. Hartleben B, Gödel M, Meyer-Schwesinger C, et al. Autophagy influences glomerular disease susceptibility and maintains podpcyte homeostasis in aging mice. *J Clin Invest*. 2010;**120**(4):1084–1096.
15. Jokinen TS, Metsähonkala L, Bergamasco, et al. Benign familial juvenile epilepsy in Lagotto Romagnolo dogs. *J Vet Intern Med*. 2007;**21**(3): 464–471.
16. Jokinen TS, Rusbridge C, Steffen F, et al. Cerebellar cortical abiotrophy in Lagotto Romagnolo dogs. *J Small Anim Pract*. 2007;**48**(8):470–473.
17. Komatsu M, Waguri S, Chiba T, et al. Loss of autophagy in the central nervous system causes neurodegeneration in mice. *Nature*. 2006;**441**(7095):880–884.
18. Kyöstilä K, Syrjä P, Jagannathan V, et al. A missense change in the *ATG4D* gene links aberrant autophagy to a neurodegenerative vacuolar storage disease. *PLoS Genet*. 2015;**11**(4):e1005169.
19. Lamb CA, Dooley HC, Tooze SA. Endocytosis and autophagy: shared machinery for degradation. *Bioessays*. 2013;**35**(1):34–45.
20. Li WW, Li J, Bao JK. Microautophagy: lesser-known self-eating. *Cell Mol Life Sci*. 2012;**69**(7):1125–1136.
21. Marino G, Uria JA, Puente XS, et al. Human autophagins, a family of cysteine proteinases potentially implicated in cell degradation by autophagy. *J Biol Chem*. 2003;**278**(6):3671–3678.
22. Menzies FM, Fleming A, Rubinsztein DC. Compromised autophagy and neurodegenerative diseases. *Nat Rev Neurosci*. 2015;**16**(6);345–357.
23. Mizushima N, Komatsu M. Autophagy: renovation of cells and tissues. *Cell*. 2011;**147**(4):728–741.
24. Mizushima N, Levine B, Cuervo AM, et al. Autophagy fights disease through cellular self-digestion. *Nature*. 2008;**451**(7182):1069–1075.
25. Mizushima N, Yoshimori T. How to interpret LC3 immunoblotting. *Autophagy*. 2007;**3**(6):542–545.
26. Murrow L, Malhotra R, Debnath J. ATG12–ATG3 interacts with Alix to promote basal autophagic flux and late endosome function. *Nat Cell Biol*. 2015; **17**(3):300–310.
27. Nakatogawa H, Ishi J, Asai E, et al. Atg4 recycles inappropriately lipidated Atg8 to promote autophagosome biogenesis. *Autophagy*. 2012; **8**(2):177–186.
28. Pengo N, Scolari M, Oliva L, et al. Plasma cells require autophagy for sustainable immunoglobulin production. *Nat Immunol*. 2013;**14**(3):298–305.
29. Schultz ML, Tecedor L, Chang M, et al. Clarifying lysosomal storage diseases. *Trends Neurosci*. 2011;**34**(8):401–410.
30. Sirois I, Groleau J, Pallet N, et al. Caspase activation regulates the extracellular export of autophagic vacuoles. *Autophagy*. 2012;**8**(6):927–937.
31. Thachil E, Hugot JP, Arbeille B, et al. Abnormal activation of autophagy-induced crinophagy in paneth cells from patients with Crohn's disease. *Gastroenterology*. 2012;**142**(5):1097–1099.
32. Torisu T, Torisu K, Lee IH, et al. Autophagy regulates endothelial cell processing, maturation and secretion of von Willebrand factor. *Nat Med*. 2013;**19**(10): 1281–1287.
33. Warren CD, Alroy J. Morphological, biochemical and molecular biology approaches for the diagnosis of lysosomal storage diseases. *J Vet Diagn Invest*. 2000;**12**(6):483–496.
34. Ylä-Anttila P, Mikkonen E, Happonen KE, et al. RAB24 facilitates clearance of autophagic compartments during basal conditions. *Autophagy*. 2015;**11**(10): 1833–1848.
35. Zhang T, Shen S, Qu J, et al. Global analysis of cellular protein flux quantifies the selectivity of basal autophagy. *Cell Rep*. 2016;**14**(10):2426–2439.